

# Organic & Biomolecular Chemistry

Accepted Manuscript



This article can be cited before page numbers have been issued, to do this please use: W. Jud, C. O. Kappe and D. Cantillo, *Org. Biomol. Chem.*, 2019, DOI: 10.1039/C9OB00456D.



This is an Accepted Manuscript, which has been through the Royal Society of Chemistry peer review process and has been accepted for publication.

Accepted Manuscripts are published online shortly after acceptance, before technical editing, formatting and proof reading. Using this free service, authors can make their results available to the community, in citable form, before we publish the edited article. We will replace this Accepted Manuscript with the edited and formatted Advance Article as soon as it is available.

You can find more information about Accepted Manuscripts in the [author guidelines](#).

Please note that technical editing may introduce minor changes to the text and/or graphics, which may alter content. The journal's standard [Terms & Conditions](#) and the ethical guidelines, outlined in our [author and reviewer resource centre](#), still apply. In no event shall the Royal Society of Chemistry be held responsible for any errors or omissions in this Accepted Manuscript or any consequences arising from the use of any information it contains.

## ARTICLE

## On the reactivity of anodically generated trifluoromethyl radicals toward aryl alkynes in organic/aqueous media

Wolfgang Jud,<sup>a,b</sup> C. Oliver Kappe,<sup>\*a,b</sup> and David Cantillo<sup>\*a,b</sup>Received 00th January 20xx,  
Accepted 00th January 20xx

DOI: 10.1039/x0xx00000x

An in-depth study of the reaction of electrochemically generated trifluoromethyl radicals with aryl alkynes in the presence of water is presented. The radicals are readily generated by anodic oxidation of sodium triflinate, an inexpensive and readily available CF<sub>3</sub> source, with concomitant reduction of water. Two competitive pathways, i.e. aryl trifluoromethylation vs oxytrifluoromethylation of the alkyne, which ultimately leads to the generation of α-trifluoromethyl ketones, have been observed. The influence of several reaction parameters on the reaction selectivity, including solvent effects, electrode material and substitution pattern on the aromatic ring of the substrate have been investigated. A mechanistic rationale for the generation α-trifluoromethyl ketones based on cyclic voltammetry data and radical trapping experiments is also presented. DFT calculations carried out at the M062X/6-311+G(d,p) level on the two competing pathways account for the observed selectivity.

## Introduction

Incorporation of perfluoroalkyl moieties to organic molecules typically enhances some of their biological properties such as metabolic stability, lipophilicity and bioavailability,<sup>1</sup> and hence represents an important type of modification in the production of agrochemicals, materials and pharmaceuticals (Fig. 1).<sup>2</sup> In the past two decades, a plethora of synthetic methods for the generation of C-C bonds between perfluoroalkyl groups and organic scaffolds have been reported.<sup>3</sup> In particular, research on the introduction of trifluoromethyl groups (CF<sub>3</sub>) has gained significant attention.<sup>4</sup> To this end, a variety of different trifluoromethyl donors have been developed, ranging from simple and inexpensive compounds, such as triflyl chloride,<sup>5</sup> trifluoroiodomethane,<sup>6</sup> trifluoromethyltrialkylsilane<sup>7</sup> and sodium triflinate<sup>8</sup> to more complex and expensive chemicals like the Umemoto's or Togni's reagents.<sup>9</sup> In particular, the generation of α-trifluoromethyl ketones, which may serve as versatile building blocks for a diverse set of CF<sub>3</sub>-containing molecules, has been subjected to intense research and is considered to be an especially challenging task.<sup>10</sup> Common synthetic protocols involve electrophilic or radical trifluoromethylations of silyl enol ethers,<sup>10–12</sup> or enamines,<sup>13</sup> which are generated as reactive intermediates from the parent ketone. Ideally, isolation of these intermediates is avoided, affording a one-pot, two step procedure.<sup>12</sup> Alternatively, α-trifluoromethyl ketones can be obtained by direct radical

trifluoromethylation of alkenes<sup>14</sup> or alkynes<sup>15</sup> in the presence of an oxidizing agent (e.g. molecular oxygen) or a hydroxyl source, respectively.

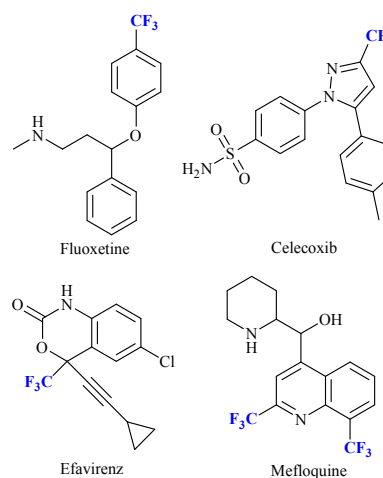


Fig. 1 Examples of CF<sub>3</sub>-containing active pharmaceutical ingredients.

Radical trifluoromethylations are typically promoted by chemical oxidation of a CF<sub>3</sub> source or photochemical methods (e.g. photoredox catalysis).<sup>4</sup> Generation of CF<sub>3</sub> radicals can also be achieved by electrochemical methods, enabling the aforementioned redox process without the need for metal- or photocatalysts or stoichiometric amounts of hazardous oxidizing or reducing agents, giving rise to highly sustainable processes.<sup>16</sup> In fact, owing to the “inherently green” character of electroorganic synthesis,<sup>17</sup> this technology has seen a considerable resurgence over the past few years. Generation of CF<sub>3</sub> radicals by anodic oxidation of several CF<sub>3</sub> sources, including CF<sub>3</sub>COOH,<sup>18</sup> CF<sub>3</sub>SO<sub>2</sub>Na,<sup>19</sup> or (CF<sub>3</sub>SO<sub>2</sub>)<sub>2</sub>Zn,<sup>20</sup> and its application for

<sup>a</sup> Institute of Chemistry, University of Graz, NAWI Graz, Heinrichstrasse 28, 8010, Graz, Austria. E-mail: oliver.kappe@uni-graz.at; david.cantillo@uni-graz.at.

<sup>b</sup> Center for Continuous Flow Synthesis and Processing (CC FLOW), Research Center Pharmaceutical Engineering GmbH (RCPE), Inffeldgasse 13, 8010 Graz, Austria. Electronic Supplementary Information (ESI) available: Supplementary Figures and Tables, copies of NMR spectra and Cartesian coordinates and energies of all calculated structures. See DOI: 10.1039/x0xx00000x



the trifluoromethylation of arenes and alkenes has been reported. Recently, we have developed a novel route for the oxytrifluoromethylation of alkenes, enabled by the electrochemical oxidation of  $\text{CF}_3\text{SO}_2\text{Na}$  in the presence of water.<sup>21</sup>

Herein, the reactivity of anodically generated  $\text{CF}_3$  radicals in organic/aqueous media is extended to more challenging aryl alkyne substrates. The rather similar nucleophilic character of the alkyne and the aromatic moiety results in competition of two reaction pathways: oxytrifluoromethylation of the alkyne, which leads to the corresponding  $\alpha$ -trifluoromethyl ketone after tautomerization of the ensuing enol, and arene trifluoromethylation (Fig. 2). In an attempt to harness reaction selectivity, the effect of several reaction parameters on product distribution has been carefully studied. Formation of  $\alpha$ -trifluoromethyl ketones was favored in most cases, although mixtures with trifluoromethyl-aryl products were always observed. DFT calculations at the M06-2X/6-311+G(d,p) level of the two competing pathways have been carried out to explain the observed selectivity.

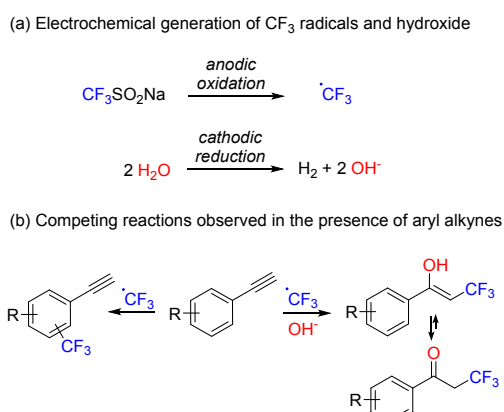


**Fig. 2** (a) Generation of  $\text{CF}_3$  radicals by anodic oxidation of sodium triflate with concomitant water reduction of water and (b) competition between oxytrifluoromethylation and aryl trifluoromethylation in the presence of aryl alkynes.

## Results and Discussion

### Aryl vs Alkyne Trifluoromethylation: Effect of Solvent Composition and Electrode Materials on Reaction Selectivity

Our investigation was carried out using 4-*tert*-butylphenylacetylene (**1a**) as model aryl alkyne. All experiments were carried out in a standardized electrochemical reactor (IKA ElectraSyn) at constant current under nitrogen atmosphere. An initial set of experiments was performed to evaluate the influence of the organic solvent, electrode material and electrolyte on the reaction outcome. All experiments were carried out on a 0.5 mmol scale, using a 0.2 M concentration for the alkyne and 1.2 equiv.  $\text{CF}_3\text{SO}_2\text{Na}$ . A constant current of 30 mA and a total charge of 2.2 F/mol (10% excess over the theoretical charge required) were applied. Notably, good to excellent conversions were obtained in all cases and, as anticipated, mixtures of the  $\alpha$ -trifluoromethyl ketone **2a** and trifluoromethyl-aryl derivatives **3a-4a** were detected by GC

analysis. Thus, in addition to the expected trifluoromethyl-aryl ketone **2a**, aryl trifluoromethylation of the  $\alpha$ -trifluoromethyl ketone **2a** (compound **4a**) was also observed. Formation of **4a** is expected to take place in the late stage of the reaction, when high concentrations of **2a** are present in the mixture (*vide infra*). Minor amounts (<5%) of trifluoromethylsulfonylated aromatics were also observed in some cases (for a GC-FID chromatogram of an example of crude reaction, see Fig. S1 in the ESI).

Using acetone as solvent, a series of anode/cathode material combinations were evaluated (Table 1, entries 1-4). While maintaining graphite as the anode, altering the cathode material (graphite, Pt, Ni, stainless steel) only had a minor influence on the reaction outcome, with **2a** being formed with highest selectivity (Table 1, entries 1-4). In contrast, complex mixtures of products were obtained with both Pt and RVC as

**Table 1** Influence of the electrode type, solvent and electrolyte on the outcome of the reaction of **1a** with  $\text{CF}_3\text{SO}_2\text{Na}$  under constant current electrolysis in organic/aqueous media.<sup>[a]</sup>

Entry	Solvent <sup>b</sup>	Anode	Cathode	Electrolyte	Conv. [%] <sup>c</sup>	<b>2a</b> [%] <sup>c</sup>	<b>3a-4a</b> [%] <sup>c</sup>
1	Acetone	Graphite	Graphite	$\text{Et}_4\text{NBF}_4$	92	63	37
2	Acetone	Graphite	Pt	$\text{Et}_4\text{NBF}_4$	93	61	25
3	Acetone	Graphite	Ni	$\text{Et}_4\text{NBF}_4$	94	67	33
4	Acetone	Graphite	SS	$\text{Et}_4\text{NBF}_4$	90	63	37
5	Acetone	RVC <sup>d</sup>	SS	$\text{Et}_4\text{NBF}_4$	99	10	20
6	Acetone	Pt	Pt	$\text{Et}_4\text{NBF}_4$	85	22	21
7	THF	Graphite	SS	$\text{Et}_4\text{NBF}_4$	51	23	53
8	MeTHF	Graphite	SS	$\text{Et}_4\text{NBF}_4$	24	35	65
9	MeCN	Graphite	SS	$\text{Et}_4\text{NBF}_4$	62	44	43
10	MeOH	Graphite	SS	$\text{Et}_4\text{NBF}_4$	73	48 <sup>e</sup>	52 <sup>f</sup>
11	$\text{CH}_2\text{Cl}_2$	Graphite	SS	$\text{Et}_4\text{NBF}_4$	99	41	31
12	Acetone	Graphite	SS	$\text{Bu}_4\text{NBF}_4$	85	62	34
13	Acetone	Graphite	SS	$\text{LiClO}_4$	85	46	37
14 <sup>g</sup>	Acetone	Graphite	SS	$\text{Et}_4\text{NBF}_4$	97	64	36
15 <sup>h</sup>	Acetone	Graphite	SS	$\text{Et}_4\text{NBF}_4$	<LOD	<LOD	<LOD

<sup>a</sup> Conditions: 0.5 mmol scale, 1.2 equiv.  $\text{CF}_3\text{SO}_2\text{Na}$ , 0.1 M electrolyte, 2.2 F/mol, constant current (30 mA) electrolysis under  $\text{N}_2$  atmosphere, 400 rpm stirring, IKA ElectraSyn 2.0 reactor. <sup>b</sup> 20:1 Mixture of the solvent and water. <sup>c</sup> Determined by GC-FID peak area integration. <sup>d</sup> Reticulated vitreous carbon. <sup>e</sup> Selectivity calculated for  $\alpha$ -trifluoromethyl methyl-enol ether (see SI for details). <sup>f</sup> Selectivity calculated for trifluoromethylation of substrate or enol ether on aromatic ring. <sup>g</sup> Constant voltage (4 V) applied. <sup>h</sup> Without electricity

anodes (Table 1, entries 5-6). This could be attributed to lower overpotentials for some undesired oxidations on Pt, or the fact



that its surface may be catalytically active for such side-reactions, and a poor mixing of the reaction mixture within the pores in the case of the RVC material.

Next, a series of solvents covering a wide range of dielectric constants were screened ( $\epsilon = 35.7$  for MeCN and  $\epsilon = 7.5$  and  $7.0$  for MeTHF and THF, respectively). The solvent choice may influence both the electrolysis efficiency, as the maximum amount of current that can be passed to the reagent solution while keeping the voltage in a 3–4 V range depends on the dielectric constant of the solvent, and the selectivity of the reaction itself. Best conversions were typically obtained in acetone. In addition, acetone favored the formation of **2a**, with a selectivity of up to 67% (Table 1, entry 3). Notably, the selectivity could be inverted in THF and MeTHF (entries 7–8). A selectivity of 65% toward aryl trifluoromethylation was observed in MeTHF as solvent (entry 8), although the reaction conversion was significantly lower than for acetone. In MeOH as solvent, an  $\alpha$ -trifluoromethyl methyl-enol ether was formed as product with 48% selectivity, resulting from methoxide acting as nucleophile instead of water (Table 1, entry 10) (see Fig. S2 in the ESI). Although full conversion was obtained in DCM, ca. 30% of an undesired, unidentified side-product was detected by GC. The type of electrolyte used had little influence on the product distribution (Table 1, entries 12–13). An additional experiment under potentiostatic conditions (constant voltage at 4 V) showed no noticeable difference with the reaction at constant current (Table 1, entry 14 vs entry 4). As expected, the reaction did not proceed in the absence of electricity, proving that an electrochemical redox process was involved in the generation of the  $\text{CF}_3$  radicals (Table 1, entry 15).

An additional set of reaction parameters, namely amount of water and  $\text{CF}_3\text{SO}_2\text{Na}$ , temperature, concentration, current and

total charge, was next investigated (Fig. 3). Conversion increased when low amounts of water were utilized (Fig. 3a). Notably, the **2a:3a-4a** ratio decreased with increasing amounts of water, and the favored product was inverted when the amount of water increased from 47 to 97 equiv. Increase of temperature, substrate concentration, amount of  $\text{CF}_3\text{SO}_2\text{Na}$  and charge had positive effects on the reaction conversion, but a less important influence on the **2a:3a-4a** product ratio (Fig. 3b–e). Low currents (Fig. 3f) favored higher **2a:3a-4a** ratios, as well as higher substrate conversion. In most cases,  $\alpha$ -trifluoromethyl ketone **2a** was the favored product of the reaction. As mentioned above, an excess of  $\text{CF}_3\text{SO}_2\text{Na}$  was required to achieve high conversions.  $^{19}\text{F}$ -NMR monitoring of the reaction mixture revealed consumption of more than one equivalent of sodium trifluoromethanesulfonate at conversions below 90%. This effect could be ascribed to trapping of some of the  $\text{CF}_3$  radicals by e.g. water and formation of volatile species.

### Effect of Substrate Substituents. Reaction Scope

To evaluate the functional group tolerance under the electrolysis conditions and assess their effect on the reaction selectivity, a diverse set of aryl alkynes was subjected to the electrochemical trifluoromethylation (Scheme 1).  $\alpha$ -Trifluoromethyl ketones **2** were favored in most cases. For that reason, derivatives **2** were isolated and characterized. Yields for **2** and the trifluoromethyl-aryl adducts **3-4** were also determined by  $^{19}\text{F}$  NMR for comparison. Since the reactions were carried out in acetone, minor amounts (< 10%) of the acetone aldol condensation products were detected in some reaction mixtures, which were likely formed under the basic conditions generated during the reaction. These impurities could easily be removed by evaporation.

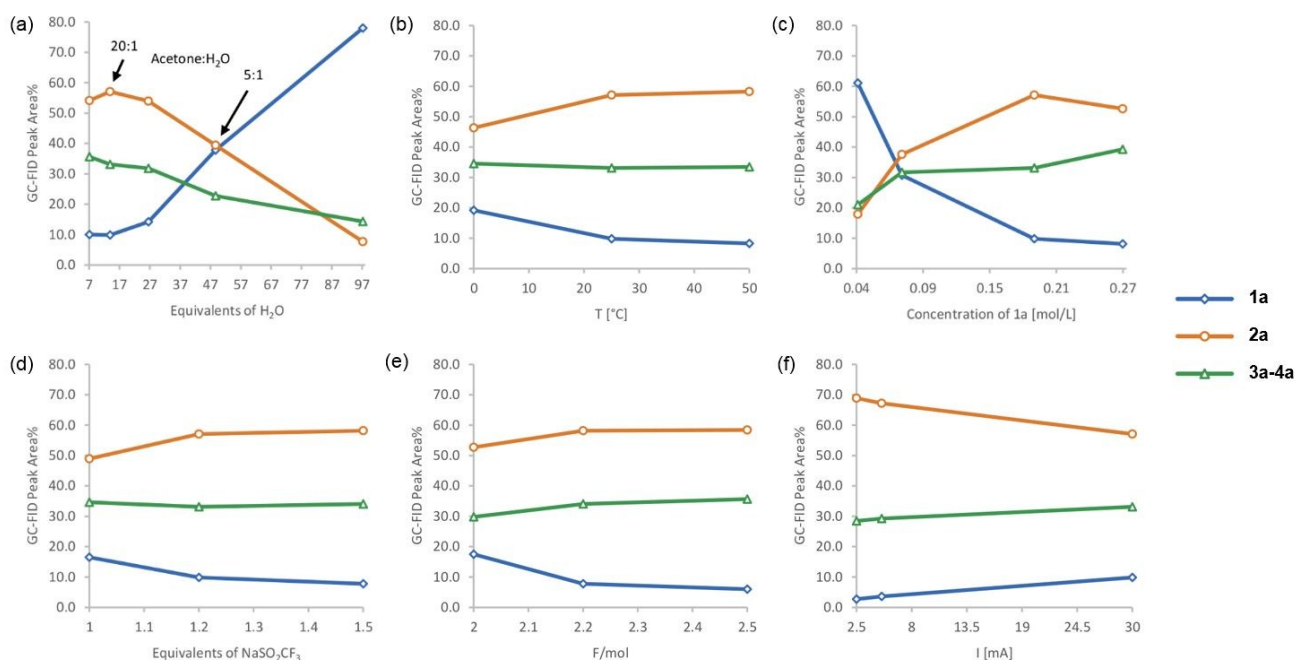
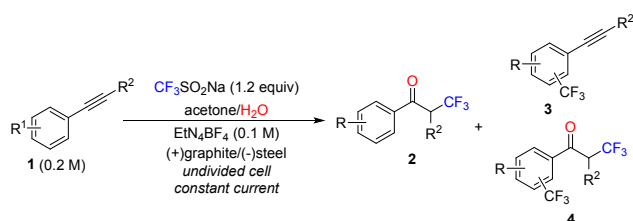


**Fig. 3** Electrochemical transformation of **1a**. Typical conditions: 0.5 mmol substrate, 1.2 equiv  $\text{CF}_3\text{SO}_2\text{Na}$ , acetone: $\text{H}_2\text{O}$  20:1 (v/v), 0.1 M  $\text{Et}_4\text{NBF}_4$ , 2.2 F/mol, constant current (30 mA), anode: graphite, cathode: stainless steel, 2.625 mL reaction volume. For a more detailed representation, including the amounts of all side products, see Fig. S3 in the ESI).



## ARTICLE

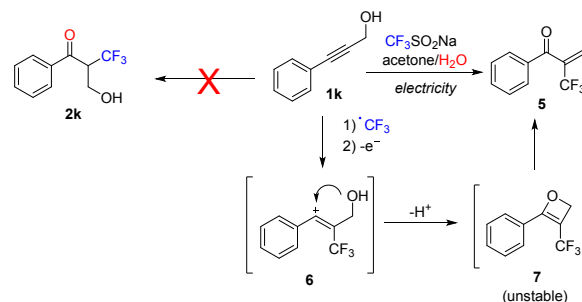
Aromatic alkynes bearing both electron withdrawing and electron donating substituents, as well as a heterocyclic aryl alkyne, were reacted with  $\text{NaSO}_2\text{CF}_3$  under electrolytic conditions (see Experimental Section for details). Surprisingly, despite the presence of deactivating functional groups on the arene in substrates **1b** and **1f**, the ratio of products did not shift in favor of the  $\alpha$ -trifluoromethyl ketone **2**. In contrast, during the reaction of the electron-rich 4-methoxyphenyl acetylene (**1e**), trifluoromethylation of the ring was clearly favored (Scheme 1). The  $\text{CF}_3$  radical addition reaction proved to be tolerant to steric effects, as both para methyl (**1h**) and ortho methyl (**1g**) phenylacetylene could be functionalized with similar yields. A non-terminal alkyne (**1j**) was also successfully derivatized under the standard reactions conditions. Notably, even the oxidatively labile substrate **1c** was converted into the  $\alpha$ -trifluoromethyl ketone **2c** in modest yield. Isolation of pure  $\alpha$ -trifluoromethyl ketones from the other reaction products was possible by simple column chromatography. Separation of **2e** from **3e** and **2j** from **3j** was problematic due to the very similar polarity of the products.



Substrate	2 (isolated yield) <sup>a</sup>	3+4 <sup>a</sup>	Substrate	2 (isolated yield) <sup>a</sup>	3+4 <sup>a</sup>
	40% (36%)	38%		26% (10%)	33%
	33% (19%)	30%		35% (29%)	37%
	12% (11%)	17%		36% (35%)	33%
	29% (27%)	34%		28% (27%)	37%
	28% (19%) <sup>b</sup>	45%		38% (–) <sup>d</sup>	9%
				– <sup>c</sup>	– <sup>c</sup>

**Scheme 1** Reaction scope for the electrochemical transformation of alkynes in the presence of  $\text{NaSO}_2\text{CF}_3$ . Conditions: 1.0 mmol substrate, 1.2 equiv.  $\text{NaSO}_2\text{CF}_3$ , Acetone:H<sub>2</sub>O 20:1 (v/v), 0.1 M  $\text{Et}_4\text{NBF}_4$ , 2.2 F/mol, constant current (15 mA), anode: graphite, cathode: stainless steel, 5 mL reaction volume <sup>a</sup> Determined by  $^{19}\text{F}$ -NMR <sup>b</sup> Essay corrected; the isolated material (32%) contained **3e**. <sup>c</sup> See Scheme 2. <sup>d</sup> Ketone **2k** could not be separated from the side products by column chromatography.

In an attempt to improve the reaction for oxidatively labile substances (e.g. **1c** and **1k**), three common oxidation mediators [triphenylamine, TEMPO and manganese(III) acetate dihydrate] were evaluated for the trifluoromethylation of these substrates as well as the model alkyne **1a**. Although a decrease of the current from 30 mA to 5 mA had a positive effect on conversion of **1a** and **1c**, the presence of mediators did not significantly change the reaction outcome (see Table S1 in the ESI). Notably, the reaction of **1k** did not afford the expected ketone **2**, but trifluoromethylacrylophenone **5** (Scheme 2). This compound is likely formed by intramolecular trapping of the carbocation intermediate **6** by the OH group (instead of water, which leads to the expected product **2**). The ensuing unstable oxetane **7** rearranges to compound **5**. Although **5** was observed in good yields (54%) by GC, its high reactivity did not allow its isolation in pure form (see Fig. S4 in the ESI).



**Scheme 2** Reaction outcome for alkyne **1j** utilizing the typical electrolysis conditions (Scheme 1).

### Proposed Mechanism for the Generation of $\alpha$ -Trifluoromethyl Ketones

Cyclic voltammograms of the starting materials (Fig. 4a) revealed that oxidation of sodium triflate occurs at 1.1 – 1.3 V (vs Ag/AgCl), and is followed by an irreversible reaction, while the model aryl alkyne substrate **1a** and even oxidatively labile alkynes require much higher oxidation potentials (2.2 – 2.5 V) (see Fig. 4a and Fig. S5 in the ESI for other alkynes). Thus, oxidation at the anode should involve the  $\text{CF}_3$  source with good selectivity.

Oxidation of triflate is known to generate  $\text{CF}_3$  radicals,<sup>8,19</sup> likely by decomposition of the initially formed  $\text{CF}_3\text{SO}_2$  radical, as pointed out by the side products observed in the reaction (see Fig. S6 in the ESI). To provide evidence for a radical reaction mechanism, we carried out a control experiment using the typical electrolysis conditions (Scheme 1) for the model substrate **1a** and using 1 equiv of butylated hydroxytoluene





(2,6-di-*tert*-butyl-4-methylphenol, BHT) as additive. Cyclic voltammetry confirmed that BHT is oxidized at

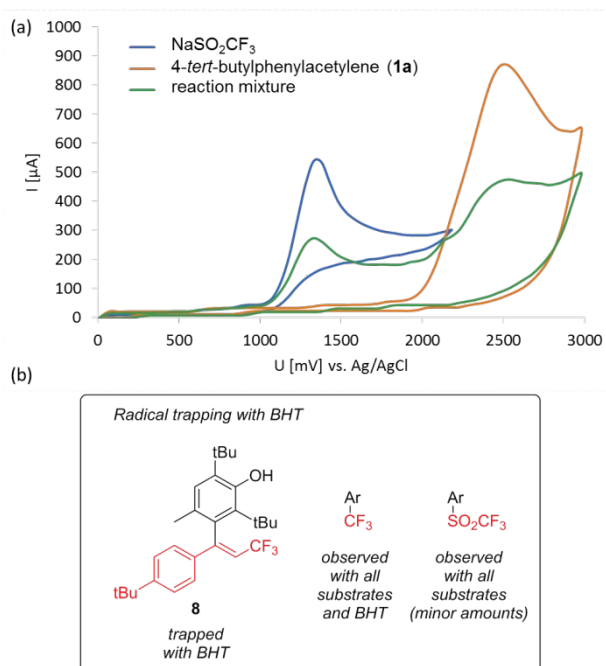


**Fig. 4** (a) Cyclic voltammograms of  $\text{CF}_3\text{SO}_2\text{Na}$ , 4-*tert*-butylphenylacetylene (**1a**) and a typical reaction mixture (see ESI for Details). (b) Species detected by GC-MS that point to the presence of the radical species highlighted in red.

higher potential than  $\text{CF}_3\text{SO}_2\text{Na}$ , and therefore it is a suitable radical trapping agent for this reaction (see Fig. S5 in the ESI). GC-MS analysis of the mixture after electrolysis revealed (see Fig. S7 in the ESI) the presence of a large amount of unreacted **1a**, confirming that BHT quenched the reaction, as well as trifluoromethylated BHT and small amounts of  $\alpha$ -trifluoromethyl ketones **2a** and **3a**. To our delight, compound **8** (Fig. 3b), corresponding to the trapping of a plausible trifluoromethylalkenyl radical, could also be detected by GC-MS analysis.

Thus, the proposed mechanism for the formation of  $\alpha$ -trifluoromethyl ketones (Fig. 5) starts with the anodic oxidation of the triflate anion, producing a trifluoromethylsulfonyl radical which decomposes into a  $\text{CF}_3$  radical and  $\text{SO}_2$ . Subsequently, the  $\text{CF}_3$  radical adds to the triple bond of the substrate in an anti-Markovnikov fashion, giving rise to the secondary alkyl radical **9** stabilized by the adjacent aromatic ring. Further oxidation of **9** produces carbocation **10**. The carbocationic species is trapped by water or the hydroxide

generated at the cathode, affording an enol ether **6**, which tautomerizes to the ketone **2**. The proposed mechanism represents an example of a paired electrochemical reaction: the hydroxide ions generated at the cathode during the electrolysis are also involved in the reaction, as one equivalent of hydroxide is incorporated in the final molecule.

### Differential Selectivity Analysis and Computational Evaluation

As described above, reactions of aryl alkynes with electrochemically generated  $\text{CF}_3$  radicals in the presence of water produced mixtures of  $\alpha$ -trifluoromethyl ketones **2** and products derived from trifluoromethylation of the aromatic ring (**3a-4a**). This occurred under all reaction conditions evaluated (Table 1, Fig. 2) and with all aryl alkynes tested (Scheme 1). Motivated by these somewhat surprising results—the reaction could not be directed to one of the two expected products, we decided to have a more detailed look into the reaction kinetics and assess the two competing pathways by DFT calculations, with the aim of providing an explanation to the observed product distribution.

HPLC monitoring of the model reaction (Fig. S8) revealed the expected formation of compounds **2a** and **3a** from the initial reaction stage, and a gradual increase in the amount of **4a** starting after 0.5 F/mol. This is due to the fact that **4a** is formed from **2a**. The reaction selectivity can be more clearly visualized by analyzing the corresponding differential selectivity plots (Fig. 6), which represent the relative amount of the reaction products at different reaction stages. Thus, the linear differential selectivity plot obtained for **2a** vs **3a** (Fig. 6a) showed that generation of the two compounds occurs simultaneously during the whole process, with a constant relative rate. The slope of the linear plot (ca. 0.32) indicated that the formation of **2a** is approximately 3 times faster than for **3a**. Selectivity values for **2a** did not match this relative rate (cf. Table 1) due to the formation of other side products (e.g. **4a**), which take place at later stages of the reaction as shown in Fig. 6b. Thus, the differential selectivity of **2a** vs the sum of all trifluoromethyl-aryl products (**3a**, **4a** and minor amounts of trifluoromethylsulfonyl derivatives) has a curved concave shape, indicating that the rate of formation of trifluoromethyl arenes increases with respect to the formation of **2a** with the reaction progress. These results were expected, as the rate of formation of **4a** is proportional to the amount of **2a** in the reaction mixture.

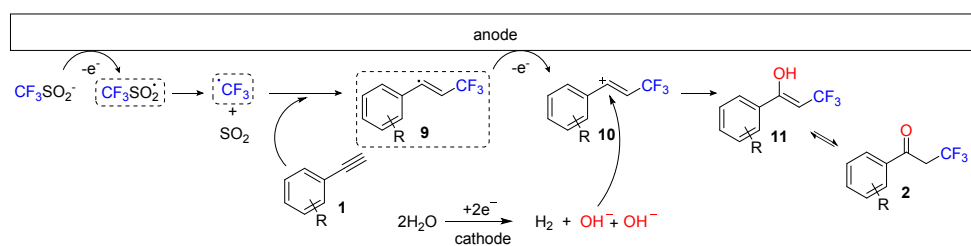


**Fig. 5** Proposed reaction mechanism for the formation of  $\alpha$ -trifluoromethyl ketones **2** from alkynes and electrochemically generated  $\text{CF}_3$  radicals in the presence of water.



## ARTICLE

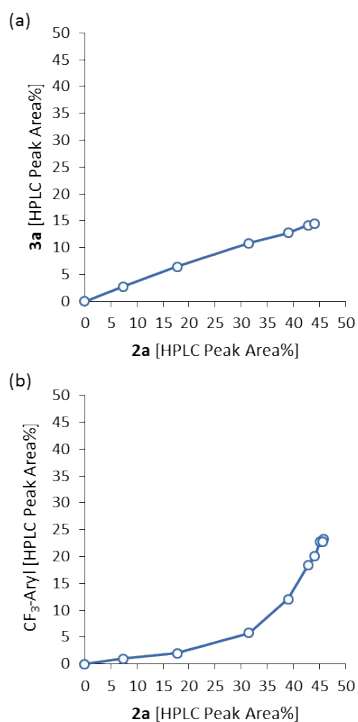


**Fig. 6** Differential selectivity plots for the formation of **2a** vs **3a** (a) and **2a** vs aryl-trifluoromethyl species (b), obtained by HPLC monitoring of the reaction mixture.

The two reaction pathways, leading to the generation of compounds **2** and **3**, were then assessed by DFT calculations to ascertain the origin of the product distribution experimentally observed. Thus, the stationary points involved in the addition of

the  $\text{CF}_3$  radical to the alkyne and aromatic ring were modelled using M06-2X functional<sup>22</sup> and the 6-311+G(d,p) basis set. All calculations incorporated solvent effects with the SMD model,<sup>23</sup> both for geometry optimization and frequency analyses, using acetone as solvent. To reduce the computational cost of the calculations, the reaction of phenyl acetylene (**1d**) was selected as model. The results were compared with the reaction of styrene (**1d'**) (Fig. 7a), which in previous studies had shown clear preference for the radical addition to the olefin in detriment of the addition to the aromatic ring.<sup>21</sup> While the reaction of the  $\text{CF}_3$  radical with the alkyne and the alkene were simply modelled for the C-2 addition, matching experimental observations, the radical addition to the aromatic ring was calculated for the ortho-, meta-, and para- positions. In the case of styrene, the two possible isomers for the ortho- and meta- addition of the  $\text{CF}_3$  radical (depending on the alkene orientation) were taken into account. The energy of the most stable isomer is presented.

The energy profile obtained for the reaction of phenyl acetylene (**1d**) with the  $\text{CF}_3$  radical (Fig. 7b, black color) revealed analogous energy barriers for all possible radical addition pathways, being all within a range of ca. 2 kcal/mol. The difference in energy between the transition state for the radical addition to the triple bond ( $\text{TS}_{1\text{d}-9\text{d}}$ ) and the most favored of the arene additions ( $\text{o-TS}_{1\text{d}-12\text{d}}$ ) was only 1.3 kcal/mol. Importantly, the similar energetics for the competing reactions satisfactorily explain the mixtures of products observed in all cases (cf. Table 1 and Fig. 2). As expected, the generation of adducts **9d** and **12d** was exergonic. 31.2 kcal/mol and 11.6–16.4 kcal/mol are released for during the formation of **9d** and **12d**, respectively.

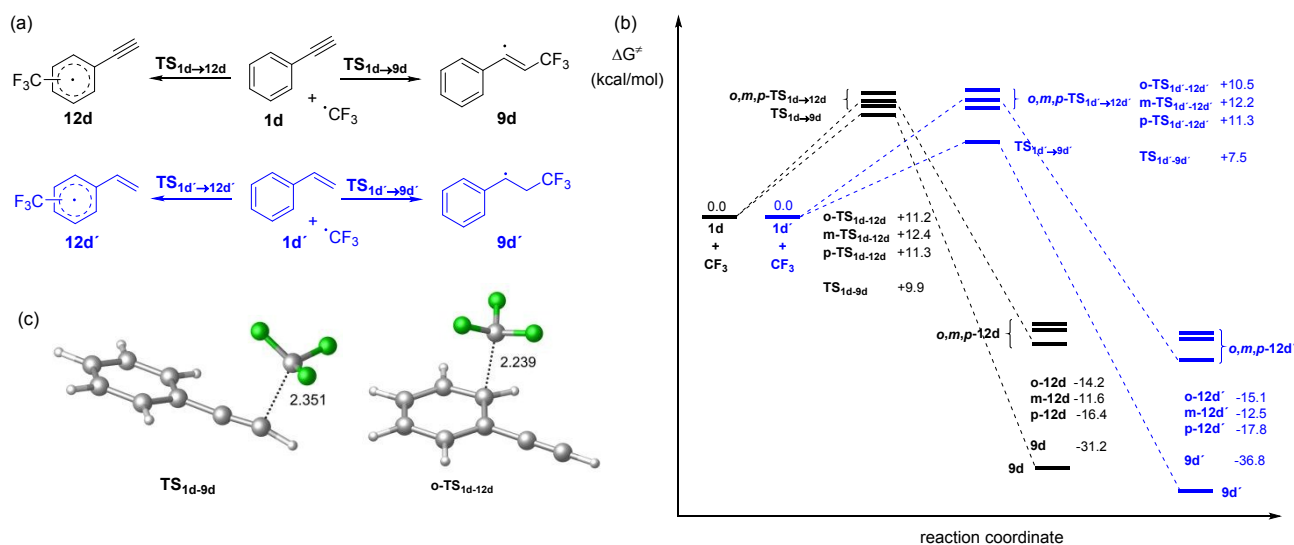


**Fig. 7** (a) Computed radical additions to the aromatic ring and the alkyne (**1d**) or alkene (**1d'**); (b) Energy profiles calculated at the M06-2X/6-311+G(d,p) level. The similar energy barriers obtained for the radical additions to the alkyne and arene of **1d** explain the mixtures of products observed experimentally; (c) structures of selected transition states.



## ARTICLE

On the other hand, the energy profile for the reaction of the  $\text{CF}_3$  radical with styrene **1d'** (Fig. 7b, blue color) presented analogous energy barriers for the addition of the radical to the arene (10.5–12.2 kcal/mol). However, the barrier for the addition to the alkene moiety resulted in significantly smaller values (7.5 kcal/mol). This difference (3 kcal/mol) accounts for the selective oxytrifluoromethylations achieved when styrene derivatives are reacted with  $\text{CF}_3$  radicals in organic aqueous media.<sup>[21]</sup> The fate of the trifluoromethylsulfonyl ( $\text{CF}_3\text{SO}_2$ ) radical that is initially formed and triggers the reaction mechanism (Fig. 5) was also modelled at the same level of theory. Notably, the calculations also predicted rapid decomposition of the radical with extrusion of  $\text{SO}_2$ , with an energy barrier of only 5.9 kcal/mol. This low barrier explained that only minor amounts of products containing the trifluoromethylsulfonyl moiety, via trapping of this radical, were observed experimentally.

## Conclusions

In summary, the present work provides a detailed experimental and theoretical study on the reactivity of electrochemically generated  $\text{CF}_3$  radicals with aryl alkynes in the presence of water. The radicals were generated by anodic oxidation of  $\text{CF}_3\text{SO}_2\text{Na}$  in an undivided cell. Similar reactivity toward radicals of the alkyne and arene moieties led to two major reaction pathways: trifluoromethylation of the aromatic ring and oxytrifluoromethylation of the alkyne. The oxytrifluoromethylation process produced a 2-trifluoromethyl enol, that upon tautomerization resulted in the formation of an  $\alpha$ -trifluoromethyl ketone. The effect on the product distribution of several reaction parameters was evaluated. Formation of  $\alpha$ -trifluoromethyl ketones was favored in most cases, except when THF or MeTHF were used as solvent. Several aryl alkynes decorated with electron-withdrawing and donating groups were tested. The reaction performed well in all cases, although always led to mixtures of products from the two competing pathways. A computational study of the radical additions to the arene and alkyne, leading to the two competing mechanisms, was carried out at the M06-2X/6-311+G(d,p) level. The analogous energy barriers calculated for all the radical additions successfully explained the selectivity observed experimentally.

## Experimental Section

**General:**  $^1\text{H}$  NMR spectra were recorded on a 300 MHz instrument.  $^{13}\text{C}$  NMR and  $^{19}\text{F}$  NMR spectra were recorded on the same instrument at 75 MHz and 282 MHz, respectively. Routine

$^{19}\text{F}$  NMR monitoring was carried out in a Magritek Spinsolve 43 benchtop NMR instrument. Chemical shifts ( $\delta$ ) are expressed in ppm downfield from TMS as internal standard. The letters s, d, t, q, and m are used to indicate singlet, doublet, triplet, quadruplet, and multiplet, respectively. GC-FID analysis was performed on a ThermoFisher Focus GC with a flame ionization detector, using a TR-5MS column (30 m  $\times$  0.25 mm ID  $\times$  0.25  $\mu\text{m}$ ) and helium as carrier gas (1 mL min<sup>-1</sup> constant flow). The injector temperature was set to 280°C. After 1 min at 50°C, the temperature was increased by 25°C min<sup>-1</sup> to 300°C and kept constant at 300°C for 4 min. The detector gases used for flame ionization were hydrogen and synthetic air (5.0 quality). GC-MS spectra were recorded using a ThermoFisher Focus GC coupled with a DSQ II (EI, 70 eV). A TR-5MS column (30 m  $\times$  0.25 mm  $\times$  0.25  $\mu\text{m}$ ) was used, with helium as carrier gas (1 mL min<sup>-1</sup> constant flow). The injector temperature was set to 280°C. After 1 min at 50°C, the temperature was increased by 25°C min<sup>-1</sup> to 300°C and kept at 300°C for 3 min. Analytical HPLC analysis was carried out on a C18 reversed-phase (RP) analytical column (150  $\times$  4.6 mm, particle size 5 mm) at 37 °C by using mobile phases A [water/acetonitrile 90:10 (v/v) + 0.1% TFA] and B (acetonitrile + 0.1% TFA) at a flow rate of 1.5 mL min<sup>-1</sup>. The following gradient was applied: linear increase from solution 30% B to 100% B in 8 min, hold at 100% solution B for 2 min. Flash chromatography purifications were carried out on an automated flash chromatography system using cartridges packed with KP-SIL, 60 Å (32–63  $\mu\text{m}$  particle size). Sodium trifluoromethanesulfonate (Code: 743232, Lot: BCBX4470), tetrabutylammonium tetrafluoroborate (Code: 217964, Lot: BCBV1430), tetraethylammonium tetrafluoroborate (Code: 242144, Lot: BCBV4670) and lithium perchlorate (Code: 634565, Lot: 0000011388) were purchased from Aldrich. All other chemicals were obtained from standard commercial vendors and were used without any further purification. Electrochemical reactions and cyclic voltammetry experiments were carried out in an IKA ElectroSyn 2.0.

**Computational details.** All calculations were carried out with the Gaussian 09 package.<sup>24</sup> The M06-2X density functional method<sup>22</sup> in conjunction with the 6-311+G(d,p) basis set was selected for all the geometry optimizations and frequency analysis. The geometries were optimized with inclusion of solvation effects. For this purpose, the SMD solvation method<sup>23</sup> was employed using acetone as solvent. Frequency calculations at 298.15 K on all stationary points were carried out at the same level of theory as the geometry optimizations to ascertain the nature of the stationary points. Ground and transition states were characterized by none and one imaginary frequency,





respectively. All of the presented relative energies are free energies at 298.15 K.

**Experimental procedure for the electrochemical transformation of aromatic alkynes on preparative Scale:** All reactions were carried out in an IKA ElectraSyn 2.0 using an IKA Graphite SK-50 anode and an IKA Stainless steel cathode. In a 5 mL IKA ElectraSyn vial, equipped with a stir bar, 0.5 mmol electrolyte (tetraethylammonium tetrafluoroborate, Et<sub>4</sub>NBF<sub>4</sub>), 1.2 mmol NaSO<sub>2</sub>CF<sub>3</sub> and 1 mmol alkyne were mixed with 5 mL Acetone and 250 µL water. After assembly of the electrochemical cell, the reaction mixtures were purged with N<sub>2</sub> for five minutes prior to switching on electricity to assure an Oxygen- and CO<sub>2</sub>-free atmosphere. The instrument was operated under constant current mode (15 mA) and 2.2 F/mol of charge were passed. After completion of the reaction, the crude product mixture was concentrated under reduced pressure and the residue was purified by flash column chromatography using as eluent petroleum ether/ethyl acetate.

**1-(4-tert-butyl)phenyl-3,3,3-trifluoropropan-1-one (2a).** 86 mg (36%); yellow oil; <sup>1</sup>H NMR (300 MHz, CDCl<sub>3</sub>) δ 7.88 (d, J = 8.1 Hz, 2H), 7.52 (d, J = 8.1 Hz, 2H), 3.77 (q, J = 10.0 Hz, 2H), 1.35 (s, 9H). <sup>13</sup>C NMR (75 MHz, CDCl<sub>3</sub>) δ 189.4, 158.3, 133.4 (d, J = 1.8 Hz), 128.4, 126.0, 124.0 (q, J = 244.5 Hz), 42.1 (q, J = 28.1 Hz), 35.4, 31.1. <sup>19</sup>F NMR (282 MHz, CDCl<sub>3</sub>) δ -61.98 (t, J = 10.1 Hz). MS-EI: m/z 229 (75%), 201 (24%), 161 (30%), 110 (100%).

**3,3,3-trifluoro-1-(4-fluorophenyl)propan-1-one (2b).** 35 mg (19%); yellow oil; <sup>1</sup>H NMR (300 MHz, CDCl<sub>3</sub>) δ 8.02 – 7.92 (m, 2H), 7.25 – 7.11 (m, 2H), 3.77 (q, J = 9.9 Hz, 2H). <sup>13</sup>C NMR (75 MHz, CDCl<sub>3</sub>) δ 188.3, 168.2, 164.8, 132.4, 131.4, 131.2, 124.0 (q, J = 277.1 Hz), 116.5, 116.2, 42.3 (q, J = 28.3 Hz). <sup>19</sup>F NMR (282 MHz, CDCl<sub>3</sub>) δ -62.03 (t, J = 10.0 Hz, 3F), -102.86 (m, 1F). MS-EI: m/z 206 (6%), 123 (100%), 95 (76%).

**4-(3,3,3-trifluoropropanoyl)benzaldehyde (2c).** 23 mg (11%); yellow oil; <sup>1</sup>H NMR (300 MHz, CDCl<sub>3</sub>) δ 10.13 (s, 1H), 8.09 (d, J = 8.4 Hz, 2H), 8.02 (d, J = 8.4 Hz, 2H), 3.85 (q, J = 9.8 Hz, 2H). <sup>13</sup>C NMR (75 MHz, CDCl<sub>3</sub>) δ 191.4, 189.3, 139.8, 130.1, 129.1, 123.8 (q, J = 276.0 Hz), 42.7 (q, J = 28.6 Hz). <sup>19</sup>F NMR (282 MHz, CDCl<sub>3</sub>) δ -62.01 (t, J = 9.8 Hz). MS-EI: m/z 216 (7%), 133 (80%), 105 (35%).

**3,3,3-trifluoro-1-phenylpropan-1-one (2d).** 47 mg (27%); yellow oil; <sup>1</sup>H NMR (300 MHz, CDCl<sub>3</sub>) δ 7.99 – 7.91 (m, 2H), 7.68 – 7.60 (m, 1H), 7.55 – 7.48 (m, 2H), 3.80 (q, J = 10.0 Hz, 2H). <sup>13</sup>C NMR (75 MHz, CDCl<sub>3</sub>) δ 189.8, 135.9, 134.4, 129.1, 128.5, 124.1 (q, J = 277.0 Hz), 42.2 (q, J = 28.2 Hz). <sup>19</sup>F NMR (282 MHz, CDCl<sub>3</sub>) δ -62.04 (t, J = 9.9 Hz). MS-EI: m/z 188 (8%), 105 (100%), 77 (86%).

**1-(4-bromophenyl)-3,3,3-trifluoropropan-1-one (2f).** 26 mg (10%); yellow oil; <sup>1</sup>H NMR (300 MHz, CDCl<sub>3</sub>) δ 7.85 – 7.75 (m, 2H), 7.70 – 7.61 (m, 2H), 3.76 (q, J = 9.9 Hz, 2H). <sup>13</sup>C NMR (75 MHz, CDCl<sub>3</sub>) δ 188.9, 134.6, 132.5, 130.0, 129.8, 123.9 (q, J = 277.1 Hz), 42.3 (q, J = 28.5 Hz). <sup>19</sup>F NMR (282 MHz, CDCl<sub>3</sub>) δ -61.99 (t, J = 9.9 Hz). MS-EI: m/z 185 (93%), 183 (100%), 157 (64%), 155 (26%), 76 (98%), 74 (81%).

**3,3,3-trifluoro-1-(o-tolyl)propan-1-one (2g).** 54 mg (29%); yellow oil; <sup>1</sup>H NMR (300 MHz, CDCl<sub>3</sub>) δ 7.65 – 7.59 (m, 1H), 7.42 – 7.47 (m, 1H), 7.31 (t, J = 7.3 Hz, 2H), 3.75 (q, J = 10.1 Hz, 2H), 2.54 (s, 3H). <sup>13</sup>C NMR (75 MHz, CDCl<sub>3</sub>) δ 192.9 (d, J = 2.4 Hz),

139.7, 136.0, 132.7, 132.6, 129.6, 129.1, 126.2, 124.1 (q, J = 277.1 Hz), 44.5 (q, J = 27.7 Hz), 21.7. <sup>19</sup>F NMR (282 MHz, CDCl<sub>3</sub>) δ -62.09 (t, J = 10.0 Hz). MS-EI: m/z 202 (10%), 119 (74%), 91 (100%).

**3,3,3-trifluoro-1-(p-tolyl)propan-1-one (2h).** 66 mg (35%); yellow oil; <sup>1</sup>H NMR (300 MHz, CDCl<sub>3</sub>) δ 7.83 (d, J = 8.3 Hz, 2H), 7.30 (d, J = 8.3 Hz, 2H), 3.77 (q, J = 10.0 Hz, 2H), 2.43 (s, 3H). <sup>13</sup>C NMR (75 MHz, CDCl<sub>3</sub>) δ 189.4 (d, J = 2.4 Hz), 145.5, 133.5 (d, J = 1.6 Hz), 129.8, 128.6, 124.2 (q, J = 275.3 Hz), 42.12 (q, J = 28.1 Hz), 21.9. <sup>19</sup>F NMR (282 MHz, CDCl<sub>3</sub>) δ -62.02 (t, J = 10.0 Hz). MS-EI: m/z 202 (11%), 119 (99%), 91 (100%).

**3,3,3-trifluoro-1-(thiophen-2-yl)propan-1-one (2i).** 47 mg (27%); yellow oil; <sup>1</sup>H NMR (300 MHz, CDCl<sub>3</sub>) δ 7.76–7.72 (m, 2H), 7.18 (dd, J = 4.9, 3.9 Hz, 1H), 3.71 (q, J = 10.1 Hz, 2H). <sup>13</sup>C NMR (75 MHz, CDCl<sub>3</sub>) δ 182.3 (d, J = 2.8 Hz), 143.3 (d, J = 2.0 Hz), 135.9, 133.6, 128.6, 123.8 (q, J = 277.3 Hz), 43.2 (q, J = 28.7 Hz). <sup>19</sup>F NMR (282 MHz, CDCl<sub>3</sub>) δ -61.94 (t, J = 10.1 Hz). MS-EI: m/z 194 (9%), 111 (100%), 83 (23%).

## Conflicts of interest

There are no conflicts to declare

## Acknowledgements

The CC FLOW Project (Austrian Research Promotion Agency FFG No. 862766) is funded through the Austrian COMET Program by the Austrian Federal Ministry of Transport, Innovation and Technology (BMVIT), the Austrian Federal Ministry of Science, Research and Economy (BMWFW), and by the State of Styria (Styrian Funding Agency SFG).

## References

- (a) J.-P. Bégue and D. Bonnet-Delphon, *Bioorganic and Medicinal Chemistry of Fluorine*, John Wiley & Sons, Hoboken, 2008; (b) *Fluorine in Medicinal Chemistry and Chemical Biology*, (Ed. I. Ojima), Wiley-VCH, Chichester, 2009.
- (a) D. O'Hagan, *Chem. Soc. Rev.*, 2008, **37**, 308–319; (b) K. Müller, C. Faeh and F. Diederich, *Science*, 2007, **317**, 1881–1886; (c) H.-J. Böhm, D. Banner, Bendels, S., M. Kansy, B. Kuhn, K. Müller, U. Obst-Sander and M. Stahl, *ChemBioChem*, 2004, **5**, 634–643.
- (a) H.-X. Song, Q.-Y. Han, C.-L. Zhao and C.-P. Zhang, *Green Chem.*, 2018, **20**, 1662–1731; (b) C. Alonso, E. Martínez de Marigorta, G. Rubiales and F. Palacios, *Chem. Rev.* 2015, **115**, 1847–1935.
- For selected recent reviews on trifluoromethylation chemistry see: (a) G.-b. Li, C. Zhang, C. Song and Y.-d. Ma, *Beilstein J. Org. Chem.*, 2018, **14**, 155–181; (b) E. H. Oh, H. J. Kim and S. B. Han, *Synthesis*, 2018, **50**, 3346–3358; (c) W. Wu and Z. Weng, *Synthesis*, 2018, **50**, 1958–1964; (d) Q. Lefebvre, *Synlett*, 2017, **28**, 19–23; (e) A. Prieto, O. Baudoin, D. Bouyssi and N. Monteiro, *Chem. Commun.*, 2016, **52**, 869–881; (f) M. Akita and T. Koike, *C. R. Chimie*, 2015, **18**, 742–751; (g) P. Gao, X.-R. Song, X.-Y. Liu and Y.-M. Liang, *Chem. Eur. J.*, 2015, **21**, 7648–7661; (h) J. Charpentier, N. Früh and A. Togni, *Chem. Rev.*, 2015, **115**, 650–682.
- D. A. Nagib and D. W. C. MacMillan, *Nature*, 2011, **480**, 224–228.



- 6 (a) Y. Itoh and K. Mikami, *Org. Lett.*, 2005, **7**, 4883-4885; (b) P. V. Pham, D. A. Nagib and D. W. C. MacMillan, *Angew. Chem. Int. Ed.*, 2011, **50**, 6119-6122.
- 7 (a) Y.-b. Wu, G.-p. Lu, T. Yuan, Z.-b. Xu, L. Wan and C. Cai, *Chem. Commun.*, 2016, **52**, 13668-13670; (b) M. Oishi, H. Kondo and H. Amii, *Chem. Commun.*, 2009, 1909-1911.
- 8 H. Guyon, H. Chachignon and D. Cahard, *Beilstein J Org Chem.* 2017, **13**, 2764-2799.
- 9 N. Shibata, A. Matsnev and D. Cahard, *Beilstein J Org Chem.* 2010, **6**, No. 65. doi:10.3762/bjoc.6.65.
- 10 K. Sato, T. Yuki, R. Yamaguchi, T. Hamano, A. Tarui, M. Omote, I. Kumadaki and A. Ando, *J. Org. Chem.*, 2009, **74**, 3815-3819.
- 11 (a) L. Li, Q.-Y. Chen and Y. Guo, *J. Org. Chem.*, 2014, **79**, 5145-5152; (b) K. Mikami, Y. Tomita, Y. Ichikawa, K. Amikura and Y. Itoh, *Org. Lett.* 2006, **8**, 4671-4673
- 12 (a) P. V. Pham, D. A. Nagib and D. W. C. MacMillan, *Angew. Chem. Int. Ed.* 2011, **50**, 6119-6122; (b) D. Cantillo, O. de Frutos, J. A. Rincón, C. Mateos and C. O. Kappe, *Org. Lett.*, 2014, **16**, 896-899.
- 13 T. Kitazume and N. Ishikawa, *J. Am. Chem. Soc.* 1985, **107**, 5186-5191.
- 14 For selected examples, see: (a) Y. Yang, Y. Liu, Y. Jiang, Y. Zhang and D. A. Vicic, *J. Org. Chem.* 2015, **80**, 6639-6648; (b) E. Yamaguchi, Y. Kamito, K. Matsuo, J. Ishihara and A. Itoh, *Synthesis* 2018, **50**, 3161-3168; (c) Y.-b. Wu, G.-p. Lu, T. Yuan, Z.-b. Xu, L. Wan and C. Cai, *Chem. Commun.* 2016, **52**, 13668-13670; (d) A. Deb, S. Manna, A. Modak, T. Patra, S. Maity and D. Maiti, *Angew. Chem. Int. Ed.* 2013, **52**, 9747-9750.
- 15 (a) A. Maji, A. Hazra and D. Maiti, *Org. Lett.*, 2014, **16**, 4524-4527; (b) Y. R. Malpani, B. K. Biswas, H. S. Han, Y.-S. Jung and S. B. Han, *Org. Lett.*, 2018, **20**, 1693-1697.
- 16 For recent reviews on the applications of electrochemistry to organic synthesis, see: (a) M. Yan, Y. Kawamata and P. S. Baran, *Chem. Rev.* 2017, **117**, 13230-13319; (b) P.-G. Echeverria, D. Delbrayelle, A. Letort, F. Nomertin, M. Perez and L. Petit, *Aldrichimica Acta*, 2018, **51**, 3-19; (c) S. R. Waldvogel, A. Wiebe, T. Gieshoff, S. Möhle, E. Rodrigo and M. Zirbes, *Angew. Chem. Int. Ed.* 2018, **57**, 5594-5619; (d) S. R. Waldvogel and B. Janza, *Angew. Chem. Int. Ed.* 2014, **53**, 7122-7123.
- 17 E. J. Horn, B. R. Rosen and P. S. Baran, *ACS Cent. Sci.* 2016, **2**, 302-308.
- 18 (a) R. N. Renaud and P. J. Champagne, *Can. J. Chem.* 1975, **53**, 529-534; (b) K. Arai, K. Watts and T. Wirth, *ChemistryOpen*, 2014, **3**, 23-28.
- 19 Many applications of electrochemical oxidation of CF<sub>3</sub>SO<sub>2</sub>Na for trifluoromethylation reactions have been recently reported, a strategy originally described by Langlois: (a) B. R. Langlois, E. Laurent and N. Roidot, *Tetrahedron Lett.* 1991, **32**, 7525-7528; (b) J.-B. Tommasino, A. Brondes, M. Médebielle, M. Thomalla, B. R. Langlois and T. Billard, *Synlett* 2002, 1697-1699.
- 20 A. G. O'Brien, A. Maruyama, Y. Inokuma, M. Fujita, P. S. Baran and D. G. Blackmond, *Angew. Chem. Int. Ed.* 2014, **53**, 11868-11871.
- 21 W. Jud, C. O. Kappe and D. Cantillo, *Chem. Eur. J.* 2018, **24**, 17234-17238.
- 22 Y. Zhao and D. G. Truhlar, *Theor. Chem. Acc.* 2008, **120**, 215-241.
- 23 A. V. Marenich, C. J. Cramer and D. G. Truhlar, *J. Phys. Chem. B* 2009, **113**, 6378-6396.
- 24 Gaussian 09, Revision A.1, M. J. Frisch, G. W. Trucks, H. B. Schlegel, G. E. Scuseria, M. A. Robb, J. R. Cheeseman, G. Scalmani, V. Barone, B. Mennucci, G. A. Petersson, H. Nakatsuji, M. Caricato, X. Li, H. P. Hratchian, A. F. Izmaylov, J. Bloino, G. Zheng, J. L. Sonnenberg, M. Hada, M. Ehara, K. Toyota, R. Fukuda, J. Hasegawa, M. Ishida, T. Nakajima, Y. Honda, O. Kitao, H. Nakai, T. Vreven, J. A. Montgomery, Jr., J. E. Peralta, F. Ogliaro, M. Bearpark, J. J. Heyd, E. Brothers, K. N. Kudin, V. N. Staroverov, R. Kobayashi, J. Normand, K. Raghavachari, A. Rendell, J. C. Burant, S. S. Iyengar, J. Tomasi, M. Cossi, N. Rega, J. M. Millam, M. Klene, J. E. Knox, J. B. Cross, V. Bakken, C. Adamo, J. Jaramillo, R. Gomperts, R. E. Stratmann, O. Yazyev, A. J. Austin, R. Cammi, C. Pomelli, J. W. Ochterski, R. L. Martin, K. Morokuma, V. G. Zakrzewski, G. A. Voth, P. Salvador, J. J. Dannenberg, S. Dapprich, A. D. Daniels, Ö. Farkas, J. B. Foresman, J. V. Ortiz, J. Cioslowski and D. J. Fox, Gaussian, Inc. Wallingford CT, 2009.



## TOC graphic and text

Two competing pathways have been experimentally observed and the selectivity explained by means of DFT calculations

